
Masked Unsupervised Self-training for Zero-shot Image Classification

Junnan Li, Silvio Savarese, Steven C.H. Hoi
{junnan.li,ssavarese,shoi}@salesforce.com

Abstract

State-of-the-art computer vision models are mostly trained with supervised learning using human-labeled images, which limits their scalability due to the expensive annotation cost. While self-supervised representation learning has achieved impressive progress, it still requires a second stage of finetuning on labeled data. On the other hand, models pre-trained with large-scale text-image supervision (e.g., CLIP) have enabled zero-shot transfer to downstream image classification tasks. However, the zero-shot performance of CLIP-like models are often insufficient for real-world adoption. In this paper, we aim to leverage the abundant unlabeled data to improve the performance of a pre-trained zero-shot classifier on downstream tasks. We propose Masked Unsupervised Self-Training (MUST), a new approach which leverages two different and complimentary sources of supervision: pseudo-labels and raw images. MUST jointly optimizes three objectives to learn both class-level global feature and pixel-level local feature and enforces a regularization between the two. We demonstrate the efficacy of MUST on 8 downstream tasks across a variety of domains, where it improves upon CLIP by a large margin and narrows the performance gap between unsupervised and supervised classification. For instance, MUST achieves a zero-shot top-1 accuracy of 77.7% on ImageNet using ViT-B, +9.4% higher than CLIP. Our code is available at <https://github.com/salesforce/MUST>.

1 Introduction

Zero-shot image classification is a challenging goal that marks the capability of a vision model to solve tasks without human supervision. Recently, vision-language pre-training (e.g. CLIP [1]) has shown promising performance on open-vocabulary zero-shot classification, where it leverages web-scale image-text pairs to train image and text encoders that can be transferred to downstream tasks through natural language prompting. However, the zero-shot performance of CLIP is often inadequate for real-world adoptions, especially when compared to models that are trained with supervised learning. On the other hand, there are abundant unlabeled data available for many tasks. In this paper, we aim to improve the performance of an open-vocabulary zero-shot classifier by finetuning it on unlabeled images from a downstream task.

Given unlabeled data, the key question is: *what is the source of supervision?* Numerous papers have attempted to answer this question. Among them, *self-training* and *self-supervised learning* are two of the most dominant approaches. In self-training [2, 3, 4], pseudo-labels are generated by a teacher model and then used to supervise task-specific training of a student model, where the student usually has an equal model size as the teacher. On the other hand, self-supervised learning methods are generally task-agnostic. Masked image modeling [5, 6, 7], which trains the model to predict missing information from masked image patches, has recently emerged as the superior self-supervised learning method for vision transformers (ViT) [8]. However, both self-training and self-supervised learning have their limitations. Self-training overly relies on the pseudo-labels as the only source

of supervision, thus is prone to overfitting to the noise in pseudo-labels. Self-supervised learning requires an additional stage of task-specific finetuning on labeled data, thus is not a one-stop solution.

In this paper, we propose Masked Unsupervised Self-Training (MUST), a simple and effective method for zero-shot¹ image classification which utilizes both pseudo-labels and raw images as two different and complementary sources of supervision. Specifically, MUST jointly optimizes three objectives to finetune a pre-trained classification model on unlabeled images: (1) Self-training objective to learn global task-specific class prediction; (2) Masked image modeling objective to learn local pixel-level information; (3) Global-local feature alignment objective to bridge the knowledge learned from the two sources of supervision.

We validate the efficacy of MUST on 8 image classification tasks across a variety of domains. Our experiments show significant improvement over the state-of-the-art method CLIP [1]. For instance, MUST achieves +9.4% increase in zero-shot top-1 accuracy on ImageNet. On certain domains, MUST can achieve comparable performance with a strong supervised learning method. We further perform extensive quantitative and qualitative analysis to examine the effect of each proposed component. We conclude with a discussion of the limitations and future directions.

2 Related Work

Zero-shot learning traditionally aims to recognize unseen classes by training the model on base classes [9, 10], where the most common approach is to utilize auxiliary information such as attributes [11] or knowledge graphs [12]. CLIP [1] popularizes a new approach for open-vocabulary zero-shot image classification by leveraging natural language supervision from web-scale datasets. Despite its impressive performance, the zero-shot accuracy of CLIP stills falls far below the supervised method in many domains. Some recent work tries to adapt CLIP to downstream tasks using labeled data [13, 14], which is less scalable compared to our unsupervised adaptation method. Our method is also orthogonal to CLIP-like research in model pre-training and can be applied to other image classification models [15, 16, 17, 18], such as LiT [19] which performs two-stage pre-training.

Self-training has shown promising progress in many domains including vision [2, 3, 20], NLP [21], and speech [22]. Our method is more closely related to the self-training approaches proposed for semi-supervised learning [23, 24, 25], where pseudo-labels on unlabeled data are used as training targets. We construct our self-training objective by following three principles: (1) *consistency regularization* [24, 26] which enforces the model to output the same prediction when the input is perturbed; (2) *entropy minimization* [27] which encourages the model to give “sharp” predictions with low entropy; (3) *prediction fairness* [25] which alleviates the model’s bias towards certain classes. Our method leverages a separate supervision signal from raw image pixels to reduce the confirmation bias in self-training, which is orthogonal to methods for pseudo-label debiasing [28, 29].

Masked image modeling, fueled by the success of vision transformers [8], recently emerged as a more appealing self-supervised representation learning method over contrastive learning [30, 31]. While some methods train the model to predict discrete tokens [5] or contextualized representations [32] for masked image patches, MAE [6] and SimMIM [7] achieve competitive performance by simply predicting the pixel values. Different from existing self-supervised learning methods which require an additional stage of supervised finetuning on labeled data, we synergically incorporate masked image modeling into self-training as a one-stage solution for zero-shot image classification.

3 Method

MUST is a simple unsupervised learning approach that adapts a pre-trained open-vocabulary classifier to a downstream task using unlabeled images. In this paper, we consider vision transformers pre-trained by CLIP [1] as the models to be adapted due to their distinctive zero-shot performance. CLIP pre-trains an image encoder and a text encoder with a contrastive loss such that paired images and texts have higher similarities in a shared embedding space. In order to perform zero-shot classification, CLIP converts a set of class names into text embeddings using ensemble of natural language prompts (*e.g.*, a photo of a {object}). During inference, it takes the dot-product between an image embedding and all text embeddings to produce the prediction logits for that image. As shown in Figure 1,

¹The term “zero-shot” refers to *using zero number of labels for a downstream task*.

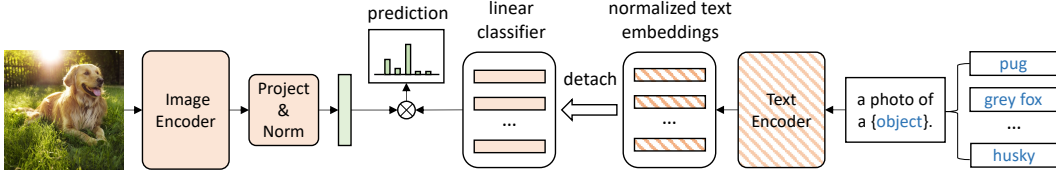


Figure 1: On each downstream task, we convert CLIP’s text embeddings into a linear classifier, which is fine-tuned together with the image encoder for unsupervised adaptation.

we convert CLIP’s non-parametric text embeddings into weights of a linear classifier, and directly finetune the linear classifier together with the image encoder for unsupervised adaptation.

Figure 2 shows the overall framework of MUST. Given an image, we follow ViT [8] to divide it into regular non-overlapping patches. A [CLS] token is appended to extract global information, which is used by the classifier for prediction. We then randomly mask image patches by replacing a patch’s embedding with a learnable [MSK] token. The output embeddings of [CLS] and [MSK] are used to jointly optimize three objectives: (1) global self-training, (2) local masked image modeling, and (3) global-local feature alignment. Next we delineate the details of each objective.

3.1 Self-training with an EMA Teacher

The self-training objective is applied to the classifier’s output. Given a batch of B unlabeled images, we compute a pseudo-label for each image by passing a weakly-augmented version of the image to a teacher model. The teacher is parameterized by an exponentially moving average (EMA) [23, 33] of the model parameters θ . Specifically, the parameters of the EMA teacher Δ are initialized as θ . During each update of θ , Δ are updated with

$$\Delta = \mu\Delta + (1 - \mu)\theta \quad (1)$$

Let q_b denote the EMA teacher’s softmax prediction for the weakly-augmented image, we enforce a cross-entropy loss against the model’s prediction p_b for a strongly-augmented version of the same image:

$$\mathcal{L}_{\text{cls}} = \frac{1}{B} \sum_{b=1}^B \mathbb{1}(\max q_b \geq \tau) \text{H}(\hat{q}_b, p_b) \quad (2)$$

Following FixMatch [24], we only use pseudo-labels with maximum scores above a threshold τ , and convert the soft labels q_b into “one-hot” hard labels by $\hat{q}_b = \arg \max(q_b)$.

Since the pseudo-labels generated by a CLIP model are often biased towards certain classes [29], minimizing \mathcal{L}_{cls} alone would magnify the bias. To prevent this, we introduce a “fairness” regularization which encourages that on average, across a batch of samples, the model predicts each class with equal frequency:

$$\mathcal{L}_{\text{reg}} = -\frac{1}{K} \sum_{k=1}^K \log(\bar{p}_k), \quad (3)$$

where K is the total number of classes, and \bar{p} is the model’s average prediction across the batch. In cases where $K > B$, we compute \bar{p} using moving average instead of batch average.

3.2 Masked Image Modeling

To alleviate the over-reliance on the noisy pseudo-labels in self-training, we introduce another source of supervision obtained from the raw images. The masked image modeling (MIM) objective aims to learn local image representation at masked positions by predicting the missing information using contextual patches. We follow SimMIM [7] and simply predict the RGB pixel values for masked patches. Specifically, given the output embedding z_b^m of the m -th [MSK] token, we first pass it through a linear decoder head to obtain the predicted RGB values $y_b^m \in \mathbb{R}^N$ for that patch, where N denotes the number of RGB pixels per patch. Then we compute the MIM loss as an ℓ_1 -loss between

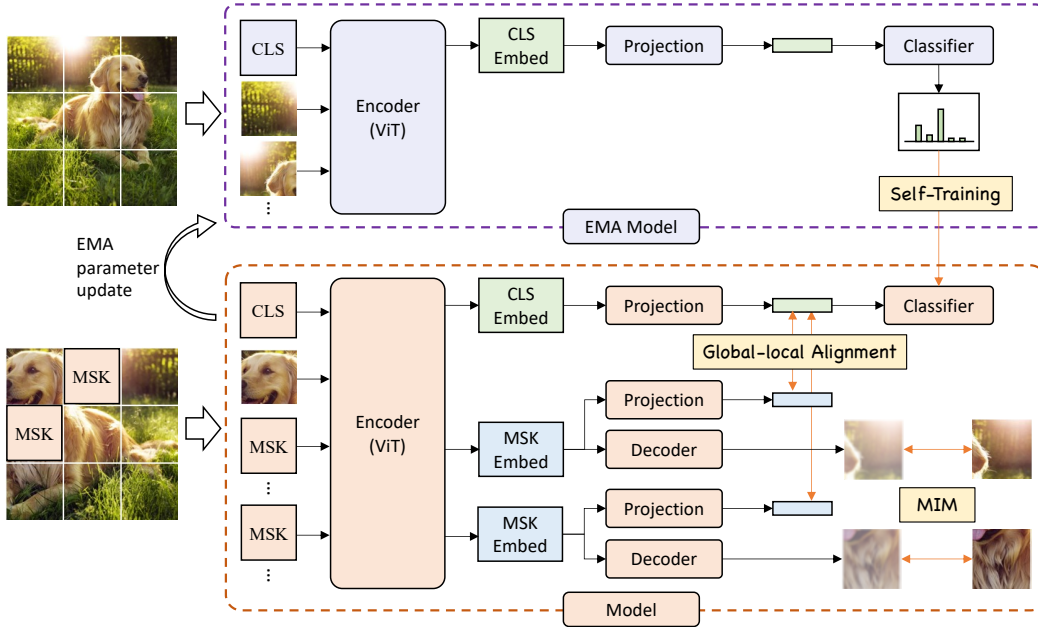


Figure 2: Unsupervised learning framework of MUST. We randomly replace image patches with [MSK] tokens, and jointly optimize three objectives on unlabeled images. (1) Global self-training: the classifier uses the output of [CLS] to predict the pseudo-label produced by an EMA model. (2) Masked image modeling: the linear decoder uses the outputs of [MSK] to predict the pixel values of the masked patches. (3) Global-local feature alignment: minimize the distance between [CLS] and [MSK] in a normalized embedding space.

y_b^m and the ground-truth RGB values x_b^m :

$$\mathcal{L}_{\text{mim}} = \frac{1}{BMN} \sum_{b=1}^B \sum_{m=1}^M \|y_b^m - x_b^m\|_1, \quad (4)$$

where M denotes the number of masked patches per image. We employ the patch-aligned random masking strategy [7] where multiple $s \times s$ patches are randomly masked with a fix masking ratio for each dataset. In general, we find that a low masking ratio (e.g., 10%) works well for most datasets, which is consistent to the observations in [7].

3.3 Global-local Feature Alignment

We aim to bridge the two sources of supervision (*i.e.*, pseudo-labels and image pixels) such that the local [MSK] features learned from MIM can improve the global [CLS] feature for better classification performance. Let z_b^c denote the output embedding of the [CLS] token, and $v_b^c = h(z_b^c)$ denote its normalized embedding after the projection network h . Following CLIP, h is a linear layer followed by ℓ_2 normalization, and v_b^c is subsequently used by the classifier to produce the prediction p_b for self-training (see Section 3.1). We also project the embeddings of the [MSK] tokens to the *same* space by passing them through h : $v_b^m = h(z_b^m)$. The global-local feature alignment loss is defined as the average squared distance between the normalized embeddings of the [CLS] token and all [MSK] tokens for each image:

$$\mathcal{L}_{\text{align}} = \frac{1}{BM} \sum_{b=1}^B \sum_{m=1}^M \|v_b^c - v_b^m\|_2^2 \quad (5)$$

During training, MUST jointly optimizes the above three objectives. The overall loss is

$$\mathcal{L} = \mathcal{L}_{\text{cls}} + \mathcal{L}_{\text{reg}} + \mathcal{L}_{\text{mim}} + \lambda \mathcal{L}_{\text{align}} \quad (6)$$

For simplicity, we only assign a tunable weight for $\mathcal{L}_{\text{align}}$ while keeping the weights for other losses as a constant of 1 across all downstream tasks.

Dataset	Train size	Test size	Metric	Description
ImageNet [37]	1,281,167	50,000	acc	1000 categories of objects from WordNet concepts
SUN397 [38]	76,129	21,758	acc	397 categories of indoor and outdoor scenes
Food101 [39]	75,750	25,250	acc	101 categories of food dishes
GTSRB [40]	26,640	12,630	acc	43 categories of German traffic signs
DTD [41]	3,760	1,880	acc	47 categories of describable textures
UCF101 [42]	9,537	3,783	acc	101 categories of human action video frames
Oxford Pets [43]	3,680	3,669	mean per class	37 categories of cats and dogs
Caltech101 [44]	3,060	6,085	mean per class	101 categories of objects and 1 background class

Table 1: Information on the image classification datasets used for transfer learning.

		ImageNet	SUN397	Food101	GTSRB	DTD	UCF101	Average
ViT-B/16	CLIP [1]	68.3	64.4	88.7	43.4	44.7	68.8	63.1
	MUST	77.7 (+9.4)	71.8 (+7.4)	92.7 (+4.0)	65.5 (+22.1)	54.1 (+9.4)	81.1 (+12.3)	73.8 (+10.8)
	Supervised	81.8 [45]	77.2	90.3	97.1	78.6	82.3	84.5
ViT-L/14	CLIP [1]	75.5	67.4	92.9	50.6	55.4	77.0	69.8
	MUST	82.1 (+6.6)	74.6 (+7.2)	95.3 (+2.4)	68.7 (+18.1)	62.6 (+7.2)	85.7 (+8.7)	78.2 (+8.4)
ViT-L/16	Supervised	83.4 [8]	81.1	93.1	97.3	79.7	86.4	86.8

Table 2: Image classification results on a variety of downstream tasks. MUST significantly improves upon CLIP for zero-shot classification on all datasets. Results for CLIP are obtained using the publicly released models. Supervised denotes the label-intensive common practice of supervised pre-training followed by supervised finetuning on downstream tasks. We use the ImageNet-1k model from [45] for supervised ViT-B and the ImageNet-21k model from [8] for supervised ViT-L.

3.4 Implementation Details

We experiment with two ViT models pre-trained by [1]: ViT-B/16 and ViT-L/14, containing respectively 12 and 24 Transformer blocks with 768 and 1024 hidden dimensions. The [MSK] token and linear decoder head are randomly initialized and finetuned together with the entire model. During finetuning, we use AdamW [34] optimizer with a weight decay of 0.05. We employ a cosine learning rate schedule without any warmup. Following [5, 6], we use a layer-wise learning rate decay [35] of 0.65 for both ViT models. The batch size is 1024 for ViT-B/16 and 512 for ViT-L/14, and the learning rate is scaled linearly with the batch size ($lr = \text{base_lr} \times \text{batchsize}/256$). We use 16 A100 GPUs, and the training process takes significantly less time compared to CLIP pre-training or self-supervised pre-training. We observe negligible variance on the results between runs with different random seeds.

The model receives input images of size 224×224 . During training, we use RandomResized-Crop+Flip+RandAug [36] to augment input images, while using Resize+RandomCrop as the weak augmentation to generate pseudo-labels. During test, we simply take a center crop after resizing the shorter edge of the image to 224. For the EMA teacher, we follow [32] and linearly ramp-up the parameter decay rate μ from μ_0 to 0.9998 in μ_n iterations. Table 9 provides more details of the hyperparameters used for each downstream task, including the pseudo-label threshold, mask patch size, mask ratio, etc.

4 Experiments

4.1 Transfer Learning Datasets

We perform experiments on 8 image classification datasets which span many different domains including common objects [37, 44], fine-grained animals [43], indoor and outdoor scenes [38], foods [39], traffic signs [40], natural textures [41], and human actions [42]. Table 1 shows the detailed information of each dataset.

4.2 MUST Results

Table 2 shows the zero-shot classification results on 6 tasks. MUST substantially improves upon CLIP on all tasks with an average accuracy improvement of **+10.8%** / **+8.4%** for ViT-B / ViT-L. We

MUST objectives	ImageNet	SUN397	Food101	GTSRB	DTD	UCF101	Average
ST+MIM+Align	77.7	71.8	92.7	65.5	54.1	81.1	73.8
ST+MIM	77.1	70.7	92.4	62.5	52.6	79.2	72.4 (-1.4)
ST	76.5	69.8	92.4	59.8	52.4	79.0	71.6 (-2.2)

Table 4: Effect of the proposed training objectives on zero-shot image classification.

Num. [MSK] for $\mathcal{L}_{\text{align}}$	ImageNet	SUN397	Food101	GTSRB	DTD	UCF101	Average
All	77.7	71.8	92.7	65.5	54.1	81.1	73.8
Nearest-10	77.6	71.9	92.7	65.7	54.1	80.8	73.8

Table 5: Number of [MSK] tokens used to align with the [CLS] token.

also experiment with a widely-adopted supervised learning approach: supervised pre-training on ImageNet (1k or 21k) followed by supervised finetuning on the downstream tasks. We finetune the ImageNet model with the same number of epochs and the same data augmentation [36] as MUST. Compared to the label-intensive supervised learning, unsupervised MUST achieves comparable performance on some datasets (e.g., Food101 and UCF101). MUST still lags behind supervised learning on some datasets (e.g., GTSRB and DTD). We hypothesize that CLIP’s low accuracy is the major cause. Since CLIP has not seen enough data from those niche domains during pre-training, its pseudo-labels would contain a limited amount of useful information. Despite this, MUST can narrow the performance gap between unsupervised and supervised learning by around 50%.

4.3 Unsupervised Transfer across Domains

Since the [MSK] token and linear decoder are trained from scratch, the potential of MUST may not be fully exploited for downstream tasks with limited number of unlabeled images. To address this, we propose to warm-up the model by training it on a similar domain with more unlabeled images. Specifically, we first employ MUST to finetune a CLIP ViT-B model on ImageNet for a single epoch, and then continue finetuning the model on two different datasets with limited number of samples (Pets and Caltech101). During warmup, we freeze the linear classifier (i.e., CLIP’s text embeddings) to anchor the normalized image embeddings in their original space for easier transfer. As shown in Table 3, warmup on ImageNet further improves the performance of MUST on both datasets.

	Pets	Caltech101
CLIP	88.9	89.8
MUST w/o ImageNet warmup	93.1 (+4.2)	93.1 (+3.3)
MUST w/ ImageNet warmup	94.3 (+5.4)	93.7 (+3.9)

Table 3: Warmup on ImageNet improves the performance of MUST on other domains.

4.4 Ablation Study

Effect of the proposed objectives. We study the effect of the three objectives: self-training, mask image modeling, and global-local feature alignment. The results are shown in Table 4. Removing the alignment loss reduces the average zero-shot accuracy by 1.4%, and removing MIM further decreases accuracy by 0.8%. The results demonstrate the importance to align the features of [CLS] and [MSK] tokens, which regularizes the model to learn better global features for classification.

Number of [MSK] tokens to align with. Our global-local feature alignment loss aims to align the [CLS] token to all of the [MSK] tokens for an image (see equation 5). We relax the alignment strength by only using the 10 [MSK] tokens that are nearest to the [CLS] token in the embedding space. As shown in Table 5, using the nearest-10 [MSK] tokens leads to similar performance compared to using all [MSK] tokens, which suggests that MUST is robust to the strength of alignment.

Effect of fairness regularization. We propose the fairness regularization loss \mathcal{L}_{reg} to counteract the bias in pseudo-labels. In Table 6, we examine its effect on the self-training objective. Our experiments use \mathcal{L}_{reg} with a constant weight of 1. The regularization improves the performance of self-training on all datasets except for SUN397 [38], which has a long-tailed class distribution in its training set. We can make \mathcal{L}_{reg} beneficial on SUN397 by simply reducing the weight of \mathcal{L}_{reg} to 0.2, which leads to a self-training accuracy of 71.4%.

	ImageNet	SUN397	Food101	GTSRB	DTD	UCF101	Average
ST w/ \mathcal{L}_{reg}	76.5	69.8	92.4	59.8	52.4	79.0	71.6
ST w/o \mathcal{L}_{reg}	74.0	71.0	91.8	50.0	46.8	73.0	67.8 (-3.8)

Table 6: Effect of the fairness regularization loss on self-training performance.



Figure 3: GradCAM visualization on validation images from multiple datasets. We visualize the self-attention from [CLS] to all patches in the last ViT layer. For each triplet, we compare three different models: CLIP (left), ST (middle), MUST (right). We make two qualitative observations: (1) MUST generally relies on more patches to make predictions; (2) MUST can better leverage the true correlation between patches and class labels.

ImageNet-C [47]	CLIP	ST	MUST	MAE+Supervised [6]
mCE ↓	70.7	55.2	53.4	51.7

Table 7: Robustness evaluation on the ImageNet-Corruption dataset.

4.5 Qualitative Analysis

MUST pays attention to more informative regions. In Figure 3, we visualize the GradCAM [46] heatmap for the self-attention from [CLS] to all patches in the last ViT layer. We compare three models - CLIP, ST, MUST- and make the following qualitative observations: (1) MUST generally relies on more patches to make predictions. E.g., the fully body of the dog instead of only the head in row 1 column 1; all four corners of the traffic sign in row 3 column 1. (2) MUST can better leverage the true correlation between image patches and class labels, instead of the spurious correlations used by CLIP and ST. E.g., the guitar is attended for the action “playing guitar” in row 4 column 1, instead of the person or the background.

A helpful MIM is not necessarily good at image recovery. In Figure 4, we show examples of recovered images from the MIM output on the validation set of different datasets. On some datasets with abundant samples (e.g., ImageNet), the model can learn to recover masked patches with high quality. On other datasets with fewer number of samples (e.g., GTSRB), the recovered images have lower quality with many artifacts. Despite the low recovery quality, the MIM objective still provides useful supervision that improves the image classification performance.

4.6 Robustness to Image Corruptions

In Table 7, we study the robustness of MUST to image corruptions. We evaluate the performance of ImageNet-finetuned models on the ImageNet-C[47] benchmark, which contains 15 corruption types with various severity. MUST is more robust than CLIP and ST, as suggested by a lower mean corruption error (mCE). The mCE of MUST is only slightly higher than a model that is first trained with self-supervised MAE [6] followed by supervised finetuning on ImageNet.

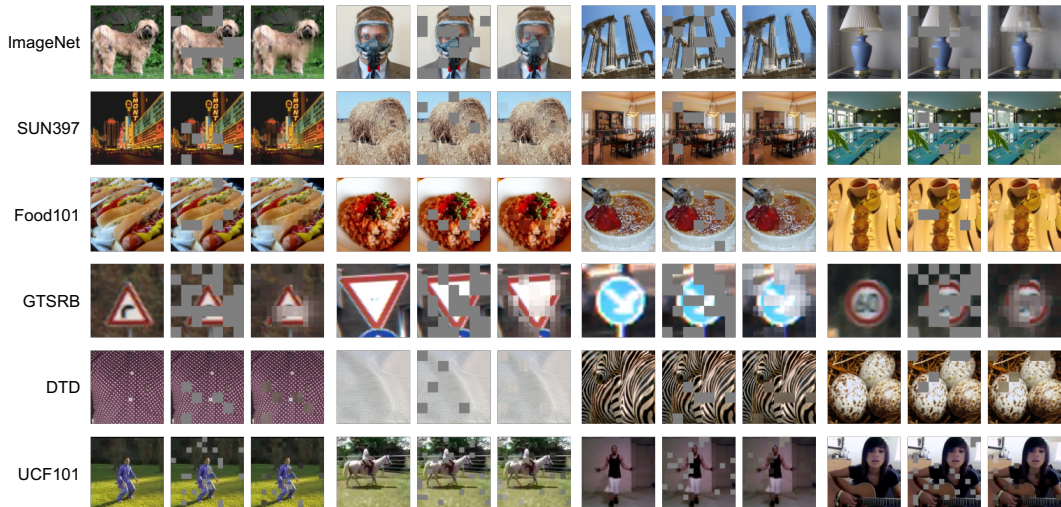


Figure 4: Examples of mask image modeling on validation images from multiple datasets. For each triplet, we show the original image (left), the masked image (middle), and the recovered image (right).

	ImageNetV2	ImageNet-R	ImageNet-A
CLIP	61.9	77.7	49.9
Inductive MUST on ImageNet	68.9 (+7.0)	68.7 (-9.0)	41.6 (-8.3)
Transductive MUST w/o ImageNet warmup	64.7 (+2.8)	87.3 (+9.6)	56.9 (+7.0)
Transductive MUST w/ ImageNet warmup	66.9 (+5.0)	87.6 (+9.9)	58.2 (+8.3)

Table 8: Evaluation of MUST under natural distribution shift from ImageNet.

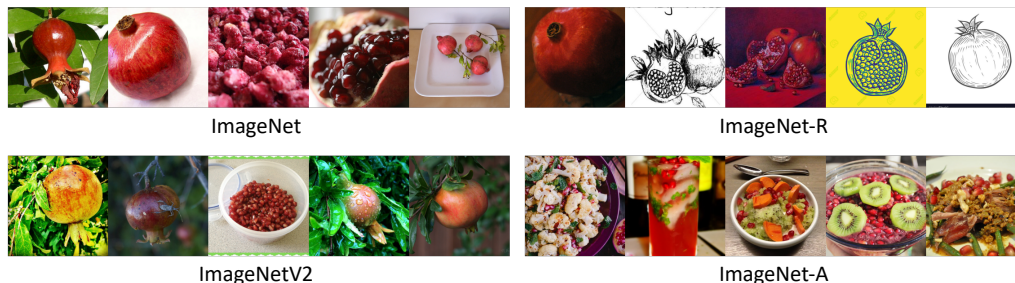


Figure 5: Example images of *pomegranate* from ImageNet and other datasets of natural distribution shifts.

4.7 Transductive Adaptation to Distribution Shift

We further investigate the robustness of MUST under natural distribution shifts. We experiment with three out-of-distribution variants of ImageNet: ImageNetV2 [48] with the same 1000 ImageNet classes, ImageNet-Rendition [49] and ImageNet-Adversarial [50] where each contains a subset of 200 classes (see Figure 5 for example images). First, we directly evaluate a ViT-B model finetuned on ImageNet using MUST, which has 77.7% accuracy on ImageNet validation set. As shown in Table 8, MUST on ImageNet improves the zero-shot classification accuracy on ImageNetV2, but decreases the performance on ImageNet-R and ImageNet-A. A similar observation is reported in CLIP [1], where supervised adaptation to ImageNet reduces the model’s average robustness to out-of-distribution datasets. To address this, we perform transductive transfer learning [9, 51] with MUST, which uses unlabeled test images from the new distribution to jointly update model parameters and infer image labels. The results in Table 8 show that transductive MUST substantially improves the model’s accuracy to distribution shift. Furthermore, the warmup on ImageNet (Section 4.3) before transductive learning leads to more improvement.

	ImageNet		SUN397		Food101		GTSRB		DTD		UCF101		Pets	Caltech101
	B	L	B	L	B	L	B	L	B	L	B	L	B	B
base lr	2e-5	4e-5	1e-4	2e-4	2e-5	4e-5	2e-5	4e-5	2e-5	4e-5	1e-5	2e-5	1e-5	1e-5
epoch	30	20	20	20	40	40	20	20	60	60	60	60	60	60
threshold τ	0.7	0.5	0.4	0.3	0.7	0.7	0.3	0.2	0.4	0.5	0.5	0.6	0.7	0.7
mask ratio	0.3	0.3	0.1	0.1	0.1	0.1	0.5	0.3	0.1	0.1	0.1	0.1	0.1	0.1
mask patch size	32	56	32	28	32	56	32	56	32	56	16	14	32	32
$\mathcal{L}_{\text{align}}$ weight λ	0.2	0.5	1	0.5	0.1	0.5	0.5	0.5	0.2	0.5	0.5	0.5	0.1	0.1
EMA init. μ_0	0.999		0.99		0.999		0.99		0.99		0.99		0.99	0.99
EMA iters. μ_n	2000		500		2000		500		100		500		100	100

Table 9: Hyperparameters for MUST on the downstream datasets. B: ViT-B/16; L: ViT-L/14.

5 Limitations and Broader Impacts

Limitations. In this paper, we show MUST as a promising domain-specific zero-shot classification algorithm where a different model is trained for each task. Although the adaptation process is efficient, the storage of additional model parameters could be a practical limitation if the number of tasks is large. There exists a simple way to address this concern: gather unlabeled image from all the domains of interest, and perform MUST to learn a single model that can generalize to multiple domains. However, this may sacrifice the model’s performance on each individual domain.

Broader Impacts. Due to the use of CLIP pre-trained models, MUST inherits some of the social implications of CLIP that arose from using minimally-filtered data crawled on the open internet, for instance, unintended leak of private information or unwanted bias. Although MUST leads to improved classification accuracy, additional analysis on the model is necessary before deploying it for real-world applications in practice.

6 Conclusion

The field of deep learning has been largely driven by simple and effective methods that can scale well. MUST is a simple method that can effectively adapt a pre-trained zero-shot classifier to downstream tasks in an unsupervised manner. The core of MUST is to simultaneously leverage two different sources of supervision signals obtained from unlabeled data: task-specific supervision from pseudo-labels and task-agnostic self supervision from raw images. We propose a simple alignment objective that bridges the two sources of supervision and enables the model to learn better features.

As a future work, MUST can be naturally extended to other domains such as NLP, where mask language modeling could act as the task-agnostic objective to improve self-training. We hope that this perspective could inspire future methods in unsupervised learning and zero-shot classification.

References

- [1] Radford, A., J. W. Kim, C. Hallacy, et al. Learning transferable visual models from natural language supervision. In M. Meila, T. Zhang, eds., *ICML*. 2021.
- [2] Zoph, B., G. Ghiasi, T. Lin, et al. Rethinking pre-training and self-training. In *NeurIPS*. 2020.
- [3] Xie, Q., M. Luong, E. H. Hovy, et al. Self-training with noisy student improves imagenet classification. In *CVPR*. 2020.
- [4] Lee, D.-H., et al. Pseudo-label: The simple and efficient semi-supervised learning method for deep neural networks. In *ICML Workshops*. 2013.
- [5] Bao, H., L. Dong, F. Wei. Beit: BERT pre-training of image transformers. In *ICLR*. 2022.
- [6] He, K., X. Chen, S. Xie, et al. Masked autoencoders are scalable vision learners. *arXiv preprint arXiv:2111.06377*, 2021.
- [7] Xie, Z., Z. Zhang, Y. Cao, et al. SimMIM: A simple framework for masked image modeling. In *CVPR*. 2022.
- [8] Dosovitskiy, A., L. Beyer, A. Kolesnikov, et al. An image is worth 16x16 words: Transformers for image recognition at scale. In *ICLR*. 2021.

- [9] Xian, Y., B. Schiele, Z. Akata. Zero-shot learning - the good, the bad and the ugly. In *CVPR*. 2017.
- [10] Wang, W., V. W. Zheng, H. Yu, et al. A survey of zero-shot learning: Settings, methods, and applications. *TIST*, 2019.
- [11] Huynh, D., E. Elhamifar. Fine-grained generalized zero-shot learning via dense attribute-based attention. In *CVPR*. 2020.
- [12] Wang, X., Y. Ye, A. Gupta. Zero-shot recognition via semantic embeddings and knowledge graphs. In *CVPR*. 2018.
- [13] Zhou, K., J. Yang, C. C. Loy, et al. Learning to prompt for vision-language models. *arXiv preprint arXiv:2109.01134*, 2021.
- [14] Gao, P., S. Geng, R. Zhang, et al. Clip-adapter: Better vision-language models with feature adapters. *arXiv preprint arXiv:2110.04544*, 2021.
- [15] Jia, C., Y. Yang, Y. Xia, et al. Scaling up visual and vision-language representation learning with noisy text supervision. *arXiv preprint arXiv:2102.05918*, 2021.
- [16] Li, Y., F. Liang, L. Zhao, et al. Supervision exists everywhere: A data efficient contrastive language-image pre-training paradigm. In *ICLR*. 2022.
- [17] Yao, L., R. Huang, L. Hou, et al. FILIP: fine-grained interactive language-image pre-training. In *ICLR*. 2022.
- [18] Li, J., C. Xiong, S. C. Hoi. Mopro: Webly supervised learning with momentum prototypes. In *ICLR*. 2021.
- [19] Zhai, X., X. Wang, B. Mustafa, et al. Lit: Zero-shot transfer with locked-image text tuning. In *CVPR*. 2022.
- [20] Sahito, A., E. Frank, B. Pfahringer. Better self-training for image classification through self-supervision. In G. Long, X. Yu, S. Wang, eds., *AI*. 2022.
- [21] He, J., J. Gu, J. Shen, et al. Revisiting self-training for neural sequence generation. In *ICLR*. 2020.
- [22] Kahn, J., A. Lee, A. Y. Hannun. Self-training for end-to-end speech recognition. In *ICASSP*, pages 7084–7088. 2020.
- [23] Tarvainen, A., H. Valpola. Mean teachers are better role models: Weight-averaged consistency targets improve semi-supervised deep learning results. In *NIPS*, pages 1195–1204. 2017.
- [24] Sohn, K., D. Berthelot, C.-L. Li, et al. Fixmatch: Simplifying semi-supervised learning with consistency and confidence. In *NeurIPS*. 2020.
- [25] Berthelot, D., N. Carlini, E. D. Cubuk, et al. Remixmatch: Semi-supervised learning with distribution alignment and augmentation anchoring. In *ICLR*. 2020.
- [26] Laine, S., T. Aila. Temporal ensembling for semi-supervised learning. In *ICLR*. 2017.
- [27] Grandvalet, Y., Y. Bengio. Semi-supervised learning by entropy minimization. In *NIPS*. 2004.
- [28] Wei, C., K. Sohn, C. Mellina, et al. Crest: A class-rebalancing self-training framework for imbalanced semi-supervised learning. In *CVPR*. 2021.
- [29] Wang, X., Z. Wu, L. Lian, et al. Debaised learning from naturally imbalanced pseudo-labels for zero-shot and semi-supervised learning. In *CVPR*. 2022.
- [30] He, K., H. Fan, Y. Wu, et al. Momentum contrast for unsupervised visual representation learning. In *CVPR*. 2020.
- [31] Chen, T., S. Kornblith, M. Norouzi, et al. A simple framework for contrastive learning of visual representations. In *ICML*. 2020.
- [32] Baeovski, A., W.-N. Hsu, Q. Xu, et al. Data2vec: A general framework for self-supervised learning in speech, vision and language. *arXiv preprint arXiv:2202.03555*, 2022.
- [33] Grill, J., F. Strub, F. Altché, et al. Bootstrap your own latent - A new approach to self-supervised learning. In H. Larochelle, M. Ranzato, R. Hadsell, M. Balcan, H. Lin, eds., *NeurIPS*. 2020.
- [34] Loshchilov, I., F. Hutter. Decoupled weight decay regularization. *arXiv preprint arXiv:1711.05101*, 2017.

- [35] Clark, K., M. Luong, Q. V. Le, et al. ELECTRA: pre-training text encoders as discriminators rather than generators. In *ICLR*. 2020.
- [36] Cubuk, E. D., B. Zoph, J. Shlens, et al. Randaugment: Practical automated data augmentation with a reduced search space. In *CVPR Workshops*. 2020.
- [37] Deng, J., W. Dong, R. Socher, et al. Imagenet: A large-scale hierarchical image database. In *CVPR*, pages 248–255. 2009.
- [38] Xiao, J., J. Hays, K. A. Ehinger, et al. SUN database: Large-scale scene recognition from abbey to zoo. In *CVPR*. 2010.
- [39] Bossard, L., M. Guillaumin, L. V. Gool. Food-101 - mining discriminative components with random forests. In D. J. Fleet, T. Pajdla, B. Schiele, T. Tuytelaars, eds., *ECCV*. 2014.
- [40] Stallkamp, J., M. Schlipsing, J. Salmen, et al. The german traffic sign recognition benchmark: A multi-class classification competition. In *IJCNN*. 2011.
- [41] Cimpoi, M., S. Maji, I. Kokkinos, et al. Describing textures in the wild. In *CVPR*. 2014.
- [42] Soomro, K., A. R. Zamir, M. Shah. Ucf101: A dataset of 101 human actions classes from videos in the wild. *arXiv preprint arXiv:1212.0402*, 2012.
- [43] Parkhi, O. M., A. Vedaldi, A. Zisserman, et al. Cats and dogs. In *CVPR*. 2012.
- [44] Binh, N. D. Online multiple tasks one-shot learning of object categories and vision. In D. Taniar, E. Pardede, H. Nguyen, J. W. Rahayu, I. Khalil, eds., *MoMM*. 2011.
- [45] Touvron, H., M. Cord, M. Douze, et al. Training data-efficient image transformers & distillation through attention. In *ICML*. 2021.
- [46] Selvaraju, R. R., M. Cogswell, A. Das, et al. Grad-cam: Visual explanations from deep networks via gradient-based localization. In *ICCV*, pages 618–626. 2017.
- [47] Hendrycks, D., T. Dietterich. Benchmarking neural network robustness to common corruptions and perturbations. *ICLR*, 2019.
- [48] Recht, B., R. Roelofs, L. Schmidt, et al. Do imagenet classifiers generalize to imagenet? In K. Chaudhuri, R. Salakhutdinov, eds., *ICML*. 2019.
- [49] Hendrycks, D., S. Basart, N. Mu, et al. The many faces of robustness: A critical analysis of out-of-distribution generalization. *ICCV*, 2021.
- [50] Hendrycks, D., K. Zhao, S. Basart, et al. Natural adversarial examples. *CVPR*, 2021.
- [51] Rohrbach, M., S. Ebert, B. Schiele. Transfer learning in a transductive setting. In C. J. C. Burges, L. Bottou, Z. Ghahramani, K. Q. Weinberger, eds., *NeurIPS*. 2013.